Localization of Curved Current Sources in Magnetocardiography

Jazbinšek V.[1], Kosch O.[2], Steinhoff U.[2], Trontelj Z.[1], and Trahms L.[2]

[1]Institute of Mathematics, Physics, and Mechanics, University of Ljubljana, Ljubljana, Slovenia
[2]Physikalisch-Technische Bundesanstalt, Berlin, Germany

Introduction

The fundamental question in the study of relation between the MCG and the ECG is whether the MCG could indicate different aspects of myocardial activity than the ECG [1]. One possibility for such activity is vortical or curved structure of the generating current distribution, which can be reflected only in MCG isofield maps. Here we applied a model of the extended curved current source for localizing the MCG source.

Method

Extended curved current sources were modeled with a constant current J along the circular arc [2], see Fig. 1. The current J is flowing from the point 1 to the point 2. The arc lies in the $x'y'$ plane of the source coordinate system S' and is determined by the starting angle α_0, length α and radius ρ. The direction of the normal $\mathbf{n}$ on the arc plane in S is defined by two angles ϑ and φ, $\mathbf{n} = (\sin\vartheta\cos\varphi, \sin\vartheta\sin\varphi, \cos\vartheta)$. Vector $\mathbf{r}'$ connects the origin of sensor coordinate system S with the origin of source coordinate system S'. The transformation from $S \rightarrow S'$ is defined with the translation by $\mathbf{r}'$, rotation by φ around z-axis and rotation by ϑ around y'-axis. The magnetic field of curved current source is calculated numerically by summation of N uniformly distributed current dipoles positioned tangentially along the arc

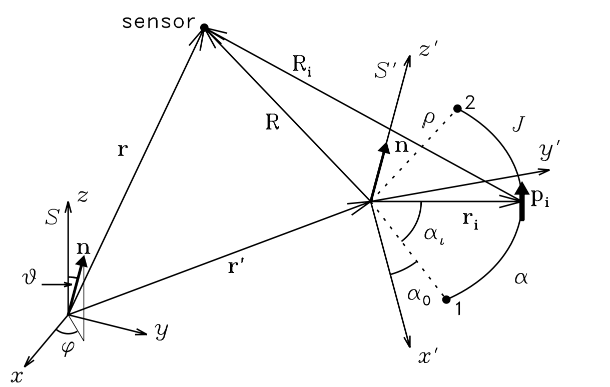

Fig. 1: Schematic representation of curved current source parameters in the sensor coordinate system S and the source coordinate system S'.

$$\mathbf{B}(\mathbf{r},\beta) = \sum_{i=1}^{N} \mathbf{B_i}(\mathbf{r},\beta) = \frac{\mu_0}{4\pi}\sum_{i=1}^{N}\frac{\mathbf{p_i}\times\mathbf{R_i}}{R_i^3}\ , \quad (1)$$

where vectors $\mathbf{R_i} = \mathbf{R} - \mathbf{r_i}$ and $\mathbf{R} = (\mathbf{r} - \mathbf{r}') = (X, Y, Z)$ connect the i-th current dipole $\mathbf{p_i}$ and the arc origin with the sensor's position, respectively (see Fig. 1). The current source is completely described by nine parameters $\beta = (\mathbf{r}', \rho, \alpha_0, \Delta\alpha, \vartheta, \varphi, p)$, where $\Delta\alpha = \alpha/N$ is the step (angle) between two successive dipoles and $p = J\rho\Delta\alpha$ is the strength of each dipole $\mathbf{p_i}$. The z-component of magnetic field (normal to the chest surface) for the i-th current dipole $\mathbf{p_i}$ is

$$\begin{aligned} B_i^z(\mathbf{r},\beta) \ = \ & \frac{\mu_0 p}{4\pi R_i^3}\Big[\cos\vartheta\sin\alpha_i(X\sin\varphi - Y\cos\varphi) \\ & - \ \cos\alpha_i(X\cos\varphi + Y\sin\varphi) + \rho\cos\vartheta\Big]. \quad (2) \end{aligned}$$

Here $\alpha_i = \alpha_0 + i\Delta\alpha$ is the polar angle of the i-th source in S' with the distance $R_i = \sqrt{R^2 + \rho^2 - 2\mathbf{R}\cdot\mathbf{r_i}}$ to the sensor, where $\mathbf{R}\cdot\mathbf{r_i}$ is expressed as

$$\begin{aligned} \mathbf{R}\cdot\mathbf{r_i} \ = \ & \rho\left[\cos\vartheta\cos\alpha_i(X\cos\varphi + Y\sin\varphi)\right. \quad (3) \\ & - \ \sin\alpha_i(X\sin\varphi - Y\cos\varphi) - Z\sin\vartheta\cos\alpha_i\left.\right]. \end{aligned}$$

We applied Levenberg-Marquardt least square algorithm [4] to find parameters β of the arc source. For comparison, we have also included in the localization procedure three other simple models (current dipole, magnetic dipole and linear source - extended current source approximated by the constant current along the straight line). We have fitted these models to measured data obtained from four healthy volunteers [3]: magnetic field in 119 B_z - channels above the chest and electric potential in 148 leads. The magnetic data were fitted using all four models, while for the electric potential data only the current dipole source model was applied. The equivalent current sources were calculated for several time instants during the QRS complex. Goodness of fit was evaluated by the root mean square (RMS) error and relative differences (RD) between measured maps and maps obtained from a model in the fitting procedure.
From MRI, which was available for one of the volunteers, we have constructed realistically shaped torso model with included the epicardium surface, see Fig. 2. All localization results were projected on axial, frontal and sagittal cross-sectional planes of the

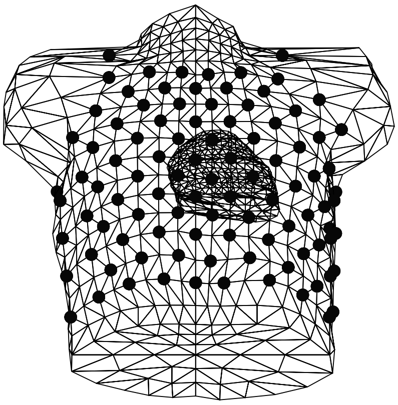

Fig. 2: Anterior view of the torso model with epicardial surface. Electrodes positions are denoted with •. Magnetic field was measured 4 cm above the chest using 119 B_z gradiometers arranged in a planar hexagonal lattice of 30 mm spacing and of 37 cm diameter.

torso model to check if the obtained equivalent current source fits into the heart region.

Results

Fig. 3 shows MCG isofield and ECG isopotential maps for two successive data sets A and B measured on one of the volunteer 15 and 20 ms after the QRS onset, respectively. The MCG maps exhibit asymmetrical pattern, especially in the case B, which is indicated by the ratio 17.4/-7.7 between maximum and minimum value. The simultaneous ECG maps reflect more symmetrical dipolar character. Figs. 4 and 5 show maps obtained by different equivalent current sources during localization procedure. As it is expected the current dipole source with its symmetrical structure cannot reproduce the measured MCG pattern, while the magnetic dipole and especially the arc source perform much better reconstruction. Table 1 displays localization results and goodness of fit obtained by different source models. For instance, RDs for the arc source are only 9.1 % and 6.3 %, RMS errors 162 fT and 350 fT in the cases A and B, respectively. The peak-to-peak values for these two maps are around 9 and 25 pT. Fig. 6 shows projections of the arc source on 3 cross-sectional planes of the torso model. Both equivalent curved current sources are situated inside the heart region in both cases A and B. In the case B, where the radius of the curved source is around 3 cm and the whole arc of length around 300°, which is almost a closed circular current loop, also the magnetic dipole has RD less then 10 % and RMS error slightly above 500 fT. For comparison, the current dipole and the linear source have for this map RD around 36% and RMS error almost 2 pT. In some other cases, not shown here, equivalent curved current sources have quite large radii (7-10 cm).

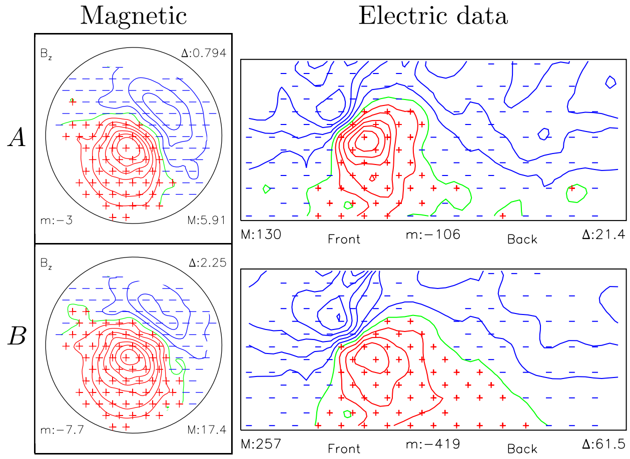

Fig. 3: MCG isofield and ECG isopotential maps for two data sets A and B, measured 15 and 20 ms after the QRS onset, respectively. Here m and M are minimal and maximal map values and Δ is the step between the two isolines. All these values are in pT for the MCG and μV for the ECG maps. Positions of measured sites are shown by + and − in accordance with the sign of measured data.

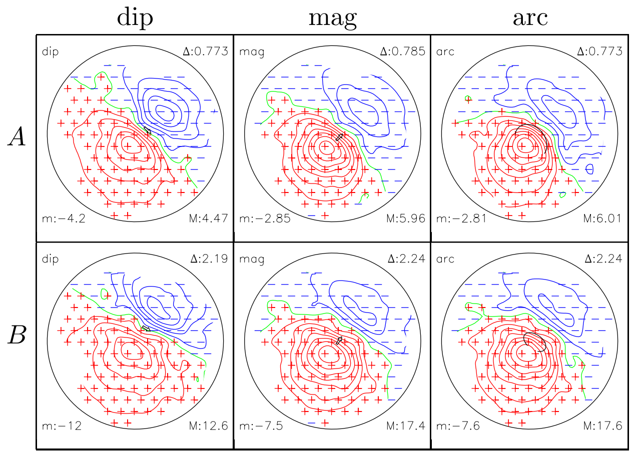

Fig. 4: MCG fitting results for A and B obtained by three source models: current dipole (dip), magnetic dipole (mag) and curved source (arc).

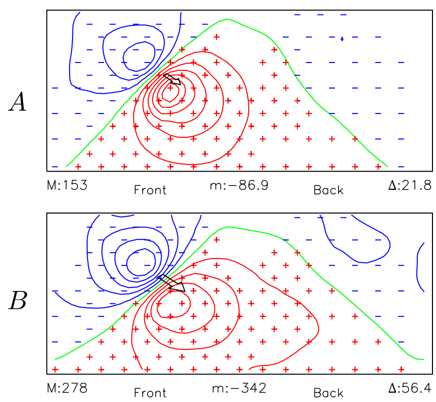

Fig. 5: ECG fitting results for A and B obtained by the current dipole source.

Table 1: Localization results and goodness of fit for two data sets A and B from Fig. 3 for different fitting functions F: the current dipole (dip), the linear source (lin), the magnetic dipole (mag) and the curved source (arc) for the magnetic data, and the current dipole (ele) for the electric data. Locations (x, y, z) are presented in the MCG sensor coordinate system with the origin in the center of the measuring xy-plane, 4 cm above the chest, where x is pointed to the left side of the thorax, y toward the head and z (depth of the source) away from the chest.

	F	x(mm)	y(mm)	z(mm)	RD(%)	RMS
	dip	30	10	-76	35.8	632 fT
	lin	31	10	-72	35.4	625 fT
A	mag	18	-5	-115	18.4	324 fT
	arc	5	-14	-98	9.1	162 fT
	ele	23	15	-110	59.0	25.6 μV
	dip	28	30	-91	35.8	1950 fT
	lin	30	29	-89	35.7	1950 fT
B	mag	17	4	-130	9.8	535 fT
	arc	13	-1	-121	6.3	346 fT
	ele	18	11	-121	49.0	61.8 μV

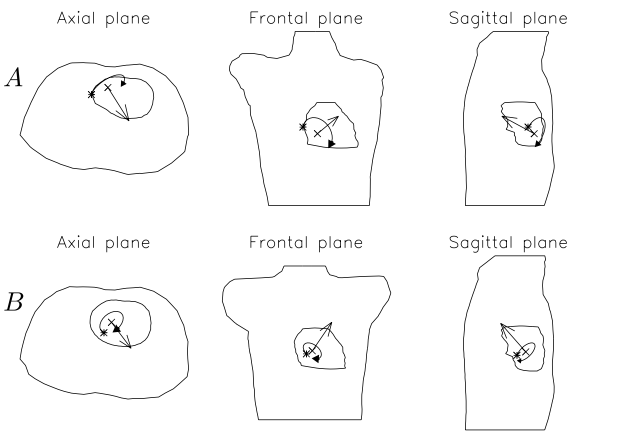

Fig. 6: Projection of curved current source on 3 cross-sectional planes of the torso model (see Fig. 2) for the two data sets A and B. Curved arrow represents current flow and the straight arrow indicates the normal to the source plane. The radius and the length of the arc are 41 mm, 204° and 29 mm, 303° in the cases A and B, respectively. The equivalent current source is in the case A positioned on the right anterior side of the epicardium while it moves deeper and sligthly to the left in the case B, where it forms almost a closed circle.

Comparison of locations obtained by different current sources in Table 1 shows that the magnetic dipole and curved current sources are close to each other, as well as locations of the current dipole and the linear source model. The distance between the localization of the magnetic dipole source to the current dipole or the linear source is smaller when the latter is fitted to electric data. In contrast to the current dipole and the linear source, the curved current source is usually localized in the heart region.

Discussion

The curved current source model gives the best result (the smallest RD and RMS error). One of the reasons for the superiority is more degrees of freedom (9) in comparison with other three source models, where only 5-6 parameters are needed for the source description. But usually not every model with only few degree of freedom more will give a better result and here the curved equivalent current source gives almost a perfect fit in some cases.

There is an essential difference between magnetic field originated from the curved source in Fig. 1 and the corresponding electric potential, which is equivalent to the electric potential generated by the straight line source connecting starting and ending points of the arc [2]. The closed arc (circle) produces no electric potential while if the radius of the circle is much smaller than the distance from the source to the sensor, the magnetic field is equivalent to the magnetic dipole source oriented parallel to the normal of the source plane.

Results of our study show that proposed model of a curved current source can be successfully applied in the localization procedure in particular in cases where the magnetic field map indicates the presence of possible vortex currents.

References

[1] Wikswo, J.P. Theoretical Aspects of the ECG-MCG Relationship, In: Samuel J. Williamson, S.J., Romani, G-L., Kaufman, L., and Modena, I. Biomagnetism: An Interdisciplinary Approach, New York, Plenum Press, 1983.

[2] Kosch, O., Steinhoff, U., Meindl, P., and Trahms, L. Physical aspects of cardiac magnetic fields and electric potentials, In: Nenonen, J., Ilmoniemi, R.J., and Katila, T. 12th Int. Conf. on Biomagnetism, Espoo, Helsinki Univ. of Technology, 2001.

[3] Jazbinsek V., Kosch, O., Meindl, P., Steinhoff, U., Trontelj, Z., and Trahms, L. Multichannel vector MFM and BSPM of chest and back, *ibid.*

[4] Press, W., Flannery, B., Teukolsky, S., and Vetterling, W. Numerical Recipes – The Art of Scientific Computing, Cambridge, Cambridge University Press, 1989.

Acknowledgments

This work was supported by the German-Slovene Bilateral Program.